A PML Solution for Vibration of Infinite Beams on Elastic Supports under Seismic Loads

Mohammadshafee Farzanian [1] and Freydoon Arbabi [2*]

1. Ph.D. Candidate, International Institute of Earthquake Engineering and Seismology (IIEES),
2. Professor, Structural Earthquake Engineering Department, IIEES,
* Corresponding Author; email: farbabi@mtu.edu

Received: 25/01/2014
Accepted: 21/05/2014

ABSTRACT

The purpose of this study is to develop a model for a class of unbounded domains with application in infinite beams on elastic supports. An unphysical layer is included in the model in order to absorb the crossing waves into the unbounded domain. To this end, the Perfectly Matched Layer (PML) is used along with a displacement-based Finite Element scheme that provides an appropriate vehicle for such problems. Most PML applications appearing in the literature have dealt with lower order governing differential equations. The case of a beam on elastic foundation, on the other hand, involves a fourth-order equation. The governing equation is reduced into a series of four first-order equations by introducing auxiliary variables. This leads to internal moments and shear forces that represent non-linear behaviour in the artificial medium. The accuracy of PML results is validated by comparison with regular finite element solutions of beams with substantially long spans. The solution method is used to investigate dynamic response of railroad tracks under earthquake excitations. The effect of various parameters on seismic response and the resonance phenomenon has been examined. Numerical results demonstrate the accuracy and efficacy of the method, which is due to use of small bounded domains in the solution process.

Keywords:
Perfectly matched layers; Infinite beams on elastic supports; Earthquake excitation

1. Introduction

Many engineering problems involve unbounded domains. Examples can be cited from quantum mechanics [1], electromagnetic waves [2], seismology [3], and soil-structure interaction [4, 5] problems. In these cases, the extent of the domain is very large when compared with the characteristic wavelength so that the solution of the wave equation requires imposition of a radiation condition in the unbounded directions. Waves radiate outwards from a source in the unbounded direction without any spurious return.

Dynamic problem of infinite beams on elastic foundations has many applications in airport runway and highway design. The application considered here is vibration of railway tracks. There are several ways to tackle such problems. Closed-form solutions of beams on elastic foundations have been derived by various researchers [6-9] in the last century. Many scientists tried to use more general solution techniques, such as boundary element methods [10, 11], finite and infinite element methods [12, 13]. For material heterogeneities or geometric irregularity, discretized procedures seem to be the only practical solution methods. Because discretization of large spatial domains can involve excessive number of elements, a number of methods have been devised

to find equivalent finite domains. Domain reduction is typically accomplished through a geometric truncation of physically bounded domain with an artificial boundary that absorbs the outgoing waves. An early paper published by Berenger [14] in 1994 introduced such absorbing boundary for the solution of wave equations. An absorbing boundary layer is a layer of artificial material placed adjacent to the edge of the grid independent of the boundary conditions. When a wave enters this absorbing layer, it is attenuated exponentially. Thus, the wave travelling through the absorbing layer is damped out upon its return. A problem with this approach arises in transition from one material to another, resulting in reflected waves. In the same manner, reflection of waves can result at the transition points of non-absorbing and absorbing materials. Berenger has shown that a special absorbing medium can be constructed for preventing reflections at interfaces. This so called perfectly matched layer (PML) was originally devised for electromagnetic problems (Maxwell equations). The same idea is applicable to other physical problems such as Helmholtz equation [15], acoustic wave propagation [16], elastic wave propagation in elastic media [17, 18], viscoelastic media [19], and in poroelastic media [20]. Basu and Chopra [21] applied the PML technique using a displacement based finite element method for one-dimensional rods on elastic supports. Kang and Kallivokas [22] used a mixed finite element formulation (displacement-stress) for the same problem. The latter two studies deal with second-order governing differential equations.

This paper deals with semi-infinite beams on elastic foundations, which involve fourth-order differential equations. Application of the PML procedure to this problem is the logical extension of the rod problem. The fourth order governing equation is reduced into a series of four first-order equations, which are then transformed in frequency domain. This leads to internal moments and shear forces that represent nonlinear behaviour in the artificial medium. The governing equations are subsequently transformed back into time domain. A weak form of the governing equations is obtained by finite element discretization. This leads to a final system of equations that is solved by a step-by-step algorithm. Numerical solution is carried out in MATLAB environment. Efficiency and accuracy of the results are validated by comparison with results of regular finite elements.

Since investigation of rail systems, as a lifeline, requires study of seismic effects [23] some researchers have considered this problem. Banimahd and Arbabi [24] used a macro-element to model the track system. They investigated seismic vulnerability and developed analytical fragility curves for railroads. An attractive alternative would be the use of PML for this problem. Another finite element model [25] has been proposed for the investigation of seismic behaviour of ballasted railway tracks and was compared with the results of a shaking table test [26]. In this model [25], an effective excited length of the track was obtained and was used to investigate the response of the track to the Kobe earthquake. Train induced vibrations can be used as an input source for artificial earthquakes [27] as well as for detection of underground effects. The PML method can facilitate the latter types of applications because of the infinite nature of these problems.

Response of railroad tracks to earthquakes, considered in this paper, provides another potential application of the PML approach. Lateral excitation of track system is considered and subjected to two different earthquake records. The influence of certain earthquakes and dynamical properties of system, the amplified rail response that is the consequence of resonance phenomenon is shown.

2. PML Formulation for Semi-Infinite Beam

2.1. Governing Differential Equations

The governing equation of motion of an infinite beam on elastic foundation, Figure (1a), can be derived by invoking the Bernoulli-Euler beam theory for the free body diagram, Figure (1b). The magnitude of the continuously distributed support reaction is proportional to the deflection of the beam. That is, the elastic foundation yields a resistive force $q(x,t) = -k_s v$.

Using equilibrium of forces and moments for the element in Figure (1b) and invoking the moment curvature relation we get the equation of motion as:

$$EI\frac{\partial^4 v}{\partial x^4} + k_s v + \rho A\frac{\partial^2 v}{\partial t^2} = p \qquad (1)$$

In this equation E is Young's modulus, I moment

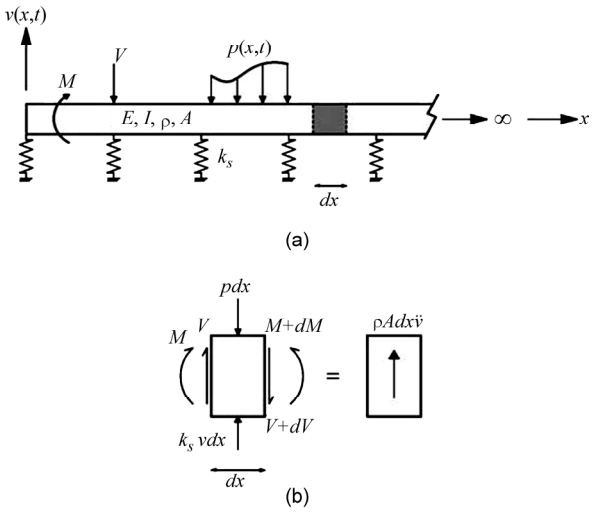

Figure 1. a) Semi-infinite beam on elastic foundation, (b) free body diagram of the beam element.

of inertia of the beam, A its cross-sectional area, ρ its density and k_s stiffness of the foundation.

2.2. Frequency Domain Equations

The PML approach has been used for longitudinal waves. Its application to the beam problem is a simple extension of the latter. Considering the time-harmonic displacement function of the form $v(x,t)=\tilde{v}(x)\exp(i\omega t)$, Eq. (1) can be transformed to frequency domain resulting in:

$$EI\frac{d^4\hat{v}}{dx^4}+k_s\hat{v}-\omega^2\rho A\hat{v}=\hat{p} \tag{2}$$

Here $\hat{v}$ is Fourier transform of the subtended function that is in terms of x, and x is the coordinate of the beam within a semi-infinite domain $0\le x<\infty$. The Fourier transform is taken with respect to t, leading to $\hat{v}$ that is a function of x only. Eq. (2) can be modified by stretching the spatial variable to complex coordinates [28]. To this end, we divide the domain into two segments; a finite domain of interest L_{BD}, and an artificial truncated domain or PML of finite length L_{PML}, Figure (2).

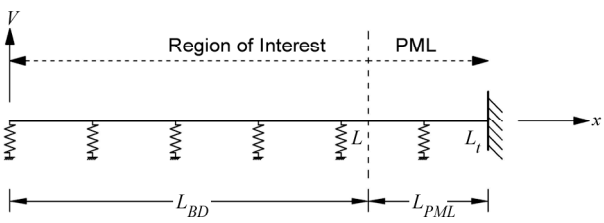

Figure 2. Truncated semi-infinite domain with a PML segment.

The solution of the semi-infinite beam has both propagating and non-propagating terms. To decay this solution within the PML and prevent wave reflections, Eq. (2) is recast by stretching the real coordinate to $\tilde{x}$ with the aid of mapping:

$$\tilde{x}=\int_0^x\lambda(s)ds \tag{3}$$

In Eq. (3), λ is a nowhere-zero, continuous complex-valued coordinate stretching function:

$$\lambda(x)=f_1(x)+\frac{1}{i\omega}f_2(x)\qquad x\in[0\ \ L_t] \tag{4}$$

where

$$f_1(x)=1+\sqrt{c/\omega r}\,f^e(x),\ \ f_2(x)=\sqrt{\omega c/r}\,f^p(x) \tag{5}$$

with

$$c=\sqrt{EI/\rho A},\quad r=\sqrt{EI/k_s} \tag{6}$$

Here c is the wave pseudo-velocity and r is the characteristic length of the beam. The so-called evanescent and propagating attenuation functions $f^e(x)$ and $f^p(x)$ are functions that must be chosen so as they will attenuate the solution of the propagating and non-propagating terms simultaneously and eliminate the wave reflections. Here they are chosen as polynomials of the form:

$$f^e(x)=f^p(x)=\begin{cases}0 & :x\in[0\ \ L_{BD}]\\ f_0\left(\dfrac{x-L_{BD}}{L_{PML}}\right)^m & :x\in[L_{BD}\ \ L_t]\end{cases} \tag{7}$$

where f_0 is the maximum value of the attenuation function and m is the degree of the polynomial function. Eq. (2) can be rewritten in terms of the stretched coordinate $\tilde{x}$, i.e. by replacing x with $\tilde{x}$. Thus the governing equation of the perfectly matched medium (PMM) becomes:

$$EI\frac{d^4\hat{v}}{d\tilde{x}^4}+k_s\hat{v}-\omega^2\rho A\hat{v}=\hat{p} \tag{8}$$

Since it is more convenient to solve the problem in terms of the real variable x, the coordinate is transformed back from the complex coordinate $\tilde{x}$. Assuming continuity of $\lambda(x)$ and invoking the chain rule of differentiation result in:

$$\frac{d}{d\tilde{x}}=\frac{1}{\lambda}\frac{d}{dx} \tag{9}$$

To proceed with the solution of the governing equation, the fourth-order differential equation is first cast into four first-order equations by introducing the following auxiliary variables

$$\hat{\phi}=\frac{1}{\lambda}\frac{d\hat{v}}{dx},\quad \hat{Y}=\frac{1}{\lambda}\frac{d\hat{\phi}}{dx},\quad \hat{q}=\frac{1}{\lambda}\frac{d\hat{Y}}{dx} \tag{10}$$

Here, rotation ϕ, curvature $Y = M/EI$ and $q = V/EI$ are in terms of x. The differential operator of Eq. (8) can be rewritten in terms of x using Eq. (9):

$$\frac{d^4}{d\tilde{x}^4}=\frac{1}{\lambda}\frac{d}{dx}\left[\frac{1}{\lambda}\frac{d}{dx}\left[\frac{1}{\lambda}\frac{d}{dx}\left(\frac{1}{\lambda}\frac{d}{dx}\right)\right]\right] \tag{11}$$

Similarly, Eq. (8) can be recast in the frequency domain by substituting the auxiliary variables into Eq. (11):

$$EI\frac{1}{\lambda}\frac{d\hat{q}}{dx}+k_s\hat{v}-\omega^2\rho A\hat{v}=\hat{p} \tag{12}$$

Multiplying both sides of Eq. (12) by $\lambda(x)$, as defined in Eq.(4), the following equation will be resulted:

$$\begin{aligned}&EI\frac{d\hat{q}}{dx}-\omega^2\rho Af_1\hat{v}+i\omega\rho Af_2\hat{v}+\\&k_sf_1\hat{v}+\frac{1}{i\omega}k_sf_2\hat{v}=\hat{p}\end{aligned} \tag{13}$$

PMM Eqs. (10) and (13) are in frequency domain and in terms of x and the auxiliary variables.

2.3. Time Domain Equations

By inverting Eq. (10) back in time domain we have:

$$\frac{\partial^2 v}{\partial x\partial t}=f_1\frac{\partial\phi}{\partial t}+f_2\phi \tag{14a}$$

$$\frac{\partial^2\phi}{\partial x\partial t}=f_1\frac{\partial Y}{\partial t}+f_2Y \tag{14b}$$

$$\frac{\partial Y}{\partial x}=f_1q+f_2\bar{q}\rightarrow q=\frac{1}{f_1}\frac{\partial Y}{\partial x}-\frac{f_2}{f_1}\bar{q} \tag{14c}$$

In this equation

$$\bar{q}=\int_0^t q(\tau)d\tau \tag{15}$$

Similarly inverse Fourier transform of Eq. (13) yields the time domain form of that equation as:

$$EI\frac{\partial q}{\partial x}+\rho Af_1\frac{\partial^2 v}{\partial t^2}+\rho Af_2\frac{\partial v}{\partial t}+k_sf_1v+k_sf_2\bar{v}=p \tag{16}$$

In this equation:

$$\bar{v}=\int_0^t v(\tau)d\tau \tag{17}$$

Thus, a set of four time domain Eqs. (14a) to (14c) and (16) with PML absorbing boundaries in the x direction can be solved by appropriate discretization schemes. Eq. (16) is implemented using the standard displacement-based finite element method and the pertinent matrices for the elements are generated by the Galerkin methods. A weak form of Eq. (16) is derived by multiplying it by an arbitrary weighting function w residing in an appropriate admissible space. Upon integration by parts over the entire computational domain Ω gives:

$$\begin{aligned}&\int_W w\rho Af_1\ddot{v}dx+\int_W w\rho Af_2\dot{v}dx+\int_W wk_sf_1v\,dx+\\&\int_W wk_sf_2\bar{v}\,dx+[wEIq]_{\partial W}=\int_W w_{,x}EIq\,dx+\int_W wp\,dx\end{aligned} \tag{18}$$

Another integration-by-parts and invoking (12.c) yields:

$$\begin{aligned}&\int_W w\rho Af_1\ddot{v}dx+\int_W w\rho Af_2\dot{v}dx+\int_W wk_sf_1v\,dx+\\&\int_W wk_sf_2\bar{v}\,dx+\int_W[w_{,x}EI\frac{1}{f_1}]_{,x}\psi dx+\int_W w_{,x}EI\frac{f_2}{f_1}\bar{q}dx=\\&\int_W wp\,dx+[w_{,x}EI\frac{1}{f_1}\psi]_{\partial W}-[wEIq]_{\partial W}\end{aligned} \tag{19}$$

2.4. Finite Element Implementation

The weak form is spatially discretized by interpolation of v and w element-wise in terms of nodal quantities using appropriate nodal shape functions. Because for fourth-order differential equations, the essential boundary conditions are the values if its first order derivatives, for a beam under flexure transverse displacement, v and rotation θ are the essential boundary conditions. Thus, these two parameters are chosen as nodal quantities leading to a simple two-node beam element with Hermitian shape functions. This leads to the system of equations:

$$\mathbf{m}\ddot{\mathbf{d}}+\mathbf{c}\dot{\mathbf{d}}+\mathbf{k}\mathbf{d}+\mathbf{k}'\bar{\mathbf{d}}+\mathbf{f}_{\text{int}}=\mathbf{f}_{ext} \tag{20}$$

with

$$\bar{\mathbf{d}}(t)=\int_0^t\mathbf{d}(\tau)d\tau \tag{21}$$

where **d** is a vector of nodal quantities. Pertinent matrices, internal and external force vectors, in the context of FEM, are assembled from the corresponding element-level matrices and vectors:

$$\mathbf{m}^e = \int_{W^e} \rho A f_1 \mathbf{N}^T \mathbf{N} dx \qquad \mathbf{c}^e = \int_{W^e} \rho A f_2 \mathbf{N}^T \mathbf{N} dx$$

$$\mathbf{k}^e = \int_{W^e} k_s f_1 \mathbf{N}^T \mathbf{N} dx \qquad \mathbf{k}'^e = \int_{W^e} k_s f_2 \mathbf{N}^T \mathbf{N} dx$$

$$\mathbf{f}^e_{ext} = \int_{W^e} \mathbf{N}^T p\, dx + \left[\mathbf{N}^T_{,x} M\right]_{\partial W^e} - \left[\mathbf{N}^T V\right]_{\partial W^e} \tag{22}$$

$$\mathbf{f}^e_{\text{int}} = \mathbf{f}^e_{\psi} + \mathbf{f}^e_{\bar{q}} \qquad \mathbf{f}^e_{\psi} = \int_{W^e} \left[\mathbf{N}^T_{,x} EI \frac{1}{f_1}\right]_{,x} \psi dx$$

$$\mathbf{f}^e_{\bar{q}} = \int_{W^e} \mathbf{N}^T_{,x} EI \frac{f_2}{f_1} \bar{q} dx$$

Here, $\mathbf{N}$ is a row vector of element-level nodal shape functions, $\mathbf{f}^e_{ext}$ is an elemental vector of external forces including distributed and concentrated loads. M and V are values of bending moment and shear force at ends of elements. $\mathbf{f}^e_{\text{int}}$ is a vector of element-level internal moments $\mathbf{f}^e_{\psi}$ plus that of internal shear forces $\mathbf{f}^e_{\bar{q}}$.

2.5. Solution Process

Step-by-step numerical integration schemes, such as the Newmark's average acceleration method can be used along with Newton-Raphson iteration at each time step to enforce the equilibrium and solve the semi-discretized system of Eq. (20). In this way, having the solution of Eq. (20) at time t_{n+1} the solution at t_n is obtained by the Newton-Raphson iteration process. This requires a) calculation of ψ_{n+1} and $\bar{q}_{n+1}$, to find $\mathbf{f}^e_{\psi_{n+1}}$ and $\mathbf{f}^e_{\bar{q}_{n+1}}$, and b) a consistent linearization [29] of $\mathbf{f}^e_{\text{int}_{n+1}}$ at $\mathbf{d}^e_{n+1}$. This is because ψ and $\bar{q}$ in Eq. (14) are in relation with displacement. Therefore, Eq. (14a) is discretized using a backward Euler scheme on ϕ to obtain:

$$\phi_{n+1} = Dr(x)[\mathbf{N}_{,x} \mathbf{d}_{n+1} + Nr(x)\phi_n] \tag{23}$$

Here, $\frac{1}{Dr(x)} = \frac{f_1}{Dt} + f_2$, $Nr(x) = \frac{f_1}{Dt}$ and Dt is the time-step. With the initial condition $\phi_1 = 0$, adding the terms of Eq. (23) together at each time step, the sequence of ϕ_{n+1} can be written in the form of a series:

$$\phi_{n+1} = \sum_{i=1}^{n+1} \frac{Nr^{(i-1)}}{Dr^{(i)}} \mathbf{N}_{,x} \mathbf{d}_{n+2-i} \tag{24}$$

Eq. (14b) is then discretized in the same fashion on ψ to obtain its series form:

$$\psi_{n+1} = \sum_{i=1}^{n+1} (i) \frac{Nr^{(i-1)}}{Dr^{(i+1)}} \mathbf{N}_{,xx} \mathbf{d}_{n+2-i} + (\frac{i}{2}) \frac{\partial}{\partial x}\left[\frac{Nr^{(i-1)}}{Dr^{(i+1)}}\right] \mathbf{N}_{,x} \mathbf{d}_{n+2-i} \tag{25}$$

The time-discrete form of element vector of internal moments is:

$$\mathbf{f}^e_{\psi_{n+1}} = \int_{W^e} \left[\mathbf{N}^T_{,x} EI \frac{1}{f_1}\right]_{,x} \psi_{n+1} dx \tag{26}$$

Linearization of Eq. (26) leads to:

$$D\mathbf{f}^e_{\psi_n} = \left[\int_{W^e} \left(\mathbf{N}^T_{,xx} D_{\psi 1} \mathbf{N}_{,xx} - \mathbf{N}^T_{,x} D_{\psi 2} \mathbf{N}_{,xx} + \mathbf{N}^T_{,xx} D_{\psi 3} \mathbf{N}_{,x} - \mathbf{N}^T_{,x} D_{\psi 4} \mathbf{N}_{,x}\right) dx\right] D\mathbf{d}_n \tag{27}$$

where D is a differential operator, and:

$$D_{\psi 1} = EI \frac{1}{Dr^2} \frac{1}{f_1}$$

$$D_{\psi 2} = EI \frac{1}{Dr^2} \frac{d}{dx}\left(\frac{1}{f_1}\right)$$

$$D_{\psi 3} = EI \frac{1}{2} \frac{d}{dx}\left(\frac{1}{Dr^2}\right) \frac{1}{f_1} \tag{28}$$

$$D_{\psi 3} = EI \frac{1}{2} \frac{d}{dx}\left(\frac{1}{Dr^2}\right) \frac{d}{dx}\left(\frac{1}{f_1}\right)$$

This linearization leads to a tangent stiffness matrix:

$$\mathbf{m}^e_{\psi} = \int_{W^e} \left(\mathbf{N}^T_{,xx} D_{\psi 1} \mathbf{N}^T_{,xx} - \mathbf{N}^T_{,x} D_{\psi 2} \mathbf{N}_{,xx} + \mathbf{N}^T_{,xx} D_{\psi 3} \mathbf{N}_{,x} - \mathbf{N}^T_{,x} D_{\psi 4} \mathbf{N}_{,x} \right) dx \tag{29}$$

The latter equation is incorporated in the effective tangent stiffness used in the time-stepping algorithm.

Derivation of $\bar{q}_{n+1}$ and internal shear force $\mathbf{f}^e_{\bar{q}_{n+1}}$ follow the same pattern. By invoking Eq. (14c) a recursive expression results in discrete form:

$$\bar{q}_{n+1} = \frac{1}{Dr} \frac{d}{dx}[\psi_{n+1}] + \frac{Nr}{Dr} \bar{q}_n \tag{30}$$

$\frac{d}{dx}[\psi_{n+1}]$ is calculated from Eq. (25) as:

$$\frac{d}{dx}[\psi_{n+1}] = \sum_{i=1}^{n+1}(i)\frac{Nr^{(i-1)}}{Dr^{(i+1)}}\mathbf{N}_{,xxx}\ddot{\mathbf{d}}_{n+2-i} + \left(\frac{3i}{2}\right)\frac{d}{dx}\left[\frac{Nr^{(i-1)}}{Dr^{(i+1)}}\right]\mathbf{N}_{,xx}\ddot{\mathbf{d}}_{n+2-i} + \left(\frac{i}{2}\right)\frac{d^2}{dx^2}\left[\frac{Nr^{(i-1)}}{Dr^{(i+1)}}\right]\mathbf{N}_{,x}\ddot{\mathbf{d}}_{n+2-i} \quad (31)$$

In the computer program developed, $\bar{q}_{n+1}$ is computed at each time-step but is dependent on the solution of all past time steps. The discretized form of the vector of internal shear forces for an element is:

$$\mathbf{f}^e_{\bar{q}_{n+1}} = \int_{W^e}\mathbf{N}^T_{,x}EI\frac{f_2}{f_1}\bar{q}_{n+1}\,dx \quad (32)$$

Linearization of Eq. (32) gives:

$$D\mathbf{f}^e_{\bar{q}_n} = \left[\int_{W^e}\left(\mathbf{N}^T_{,x}D_{\bar{q}1}\mathbf{N}_{,xxx} + \mathbf{N}^T_{,x}D_{\bar{q}2}\mathbf{N}_{,xx} + \mathbf{N}^T_{,x}D_{\bar{q}3}\mathbf{N}_{,x}\right)dx\right]D\ddot{\mathbf{d}}_n \quad (33)$$

where D is a differential operator, and:

$$D_{\bar{q}1} = EI\frac{1}{Dr^3}\frac{f_2}{f_1};$$

$$D_{\bar{q}2} = EI\frac{1}{Dr}\frac{3}{2}\frac{d}{dx}\left(\frac{1}{Dr^2}\right); \quad (34)$$

$$D_{\bar{q}3} = EI\frac{1}{Dr}\frac{1}{2}\frac{d^2}{dx^2}\left(\frac{1}{Dr^2}\right)\frac{f_2}{f_1}$$

Linearization gives the tangent matrix:

$$\mathbf{m}^e_{\bar{q}} = \int_{W^e}\left(\mathbf{N}^T_{,x}D_{\bar{q}1}\mathbf{N}_{,xxx} + \mathbf{N}^T_{,x}D_{\bar{q}2}\mathbf{N}_{,xx} + \mathbf{N}^T_{,x}D_{\bar{q}3}\mathbf{N}_{,x}\right)dx \quad (35)$$

The latter equation is incorporated in the effective tangent stiffness used in the time-stepping algorithm.

Besides, the time-integral of **d**, Eq. (21), can be approximated as:

$$\bar{\mathbf{d}}_{n+1} = \bar{\mathbf{d}}_n + \mathbf{d}_{n+1}Dt \quad (36)$$

Therefore, the terms involving $\bar{\mathbf{d}}$ in Eq. (20) may be linearized as:

$$D(\mathbf{k}'\bar{\mathbf{d}}_{n+1}) = (\mathbf{k}'Dt)D\mathbf{d}_n \quad (37)$$

The effective internal forces for each element in the Newmark scheme can be written as:

$$\mathbf{m}^e_{eff_{n+1}} = \mathbf{m}^e\ddot{\mathbf{d}}_{n+1} + \mathbf{c}^e\dot{\mathbf{d}}_{n+1} + \mathbf{k}^e\mathbf{d}_{n+1} + \mathbf{k}'^e\bar{\mathbf{d}}_{n+1} + \mathbf{f}^e_{\psi_{n+1}} + \mathbf{f}^e_{\bar{q}_{n+1}} \quad (38)$$

And the tangent stiffness matrix becomes:

$$\mathbf{k}^e_{eff} = (\mathbf{k}^e + \mathbf{k}'^eDt) + \frac{\gamma}{\beta Dt}\mathbf{c}^e + \frac{1}{\beta Dt^2}(\mathbf{m}^e + \mathbf{m}^e_{\psi} + \mathbf{m}^e_{\bar{q}}) \quad (39)$$

It should be noted that the tangent stiffness $\mathbf{k}^e_{eff}$ is independent of the solution process and can thus be computed only once. However, the internal force vector $\mathbf{f}^e_{eff_{n+1}}$ has to be recomputed at each time step because it is dependent on the solution at the previous steps.

3. Model Validation

To validate the PML model, a concentrated harmonic load, in the form of $V(0, t) = P_0\sin(0.35t)$, was applied at the origin of semi-infinite beam on elastic foundations. Here, P_0 is the load amplitude, and $\omega = 0.35$ is the frequency of excitation. Since values of deflection and slope at any point along the beam tend to zero at large distances from the origin, a comparison with beams of finite length has been made. The semi-infinite beam solution yields reasonable results for beams as short as $L_{LB} = 3\pi/2C_0$ with $C_0 = \sqrt[4]{k_s/4EI}$ [30]. The accuracy of the PML process for semi-infinite beams resting on elastic foundations was compared with the results of regular finite element analyses of a beam with length L_{LB} and fixed end conditions, Figure (3). The PML model had a length of $L_{BD} = 0.10L_{LB}$ and sufficient mesh density. At low frequencies, the maximum deflection of the beam can be computed by a static analysis as well as by the finite element model. The maximum deflection, $v_{\max}$ ($x = 0$), in the static case [30] is:

$$v_{\max}(x=0)\frac{2P_0C_0}{k_s} \quad (40)$$

Figure (3) depict results for five different values of k_s and P_0. It can be seen that the PML results are indistinguishable from the regular finite element

results in all cases.

Other properties of the aforementioned unbounded dynamical system are given below:

$$E = 200\times10^{9}[N/m^{2}],\ I = 2000\times10^{-8}[m^{4}],$$
$$\rho = 8000[kg/m^{3}],\ A = 65\times10^{-4}[m^{2}]$$

4. Earthquake Excitations

Seismic analyses are becoming part of railroad designs. The complex nature of rail systems, its theoretically infinite length can be modeled with many elements; making it difficult to simulate the whole unbounded dynamical systems. The PML model developed and applied in this study can overcome such difficulties. In the present study, only impact of the horizontal component of earthquake is considered.

Assuming the direction of the earthquake to be perpendicular to the rail axis, the equivalent seismic load vector is the product of the mass matrix with the ground acceleration. The two earthquake records considered here are that of the El Centro (US-1979) and Kocaeli (Turkey-1999). The peak ground accelerations (PGA) were normalized to 0.4 g, Figure (4). The ballasted track can have nonlinear lateral resistance [31]. However, only linear behavior is considered here and the quake was equally applied to the full length of the track model. The stiffness of the rail and the subgrade was expressed by an equivalent distributed spring. The mass of the rail, travers and the ballast was further indicated by an equivalent value.

Both soft and hard soils [32] were considered in the parametric study. To determine the effect of the ballast mass on the system, track models with rail mass only (C1) and ballast mass included (C2) were examined. Variations of the parameters, mass, lead to different first natural frequencies, as well as consideration of soft and hard soils. In these simple

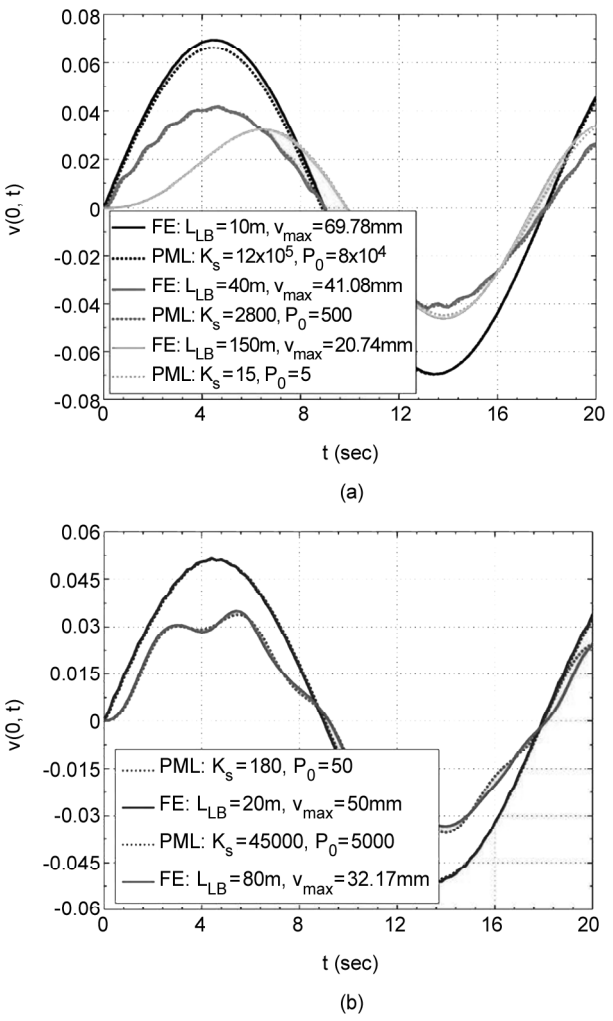

Figure 3. Nodal response of beam on elastic foundation for five different values of foundation stiffness and load amplitude: (a) k_s = 12 x 105, 2800, 15 and (b) k_s = 45000, 180.

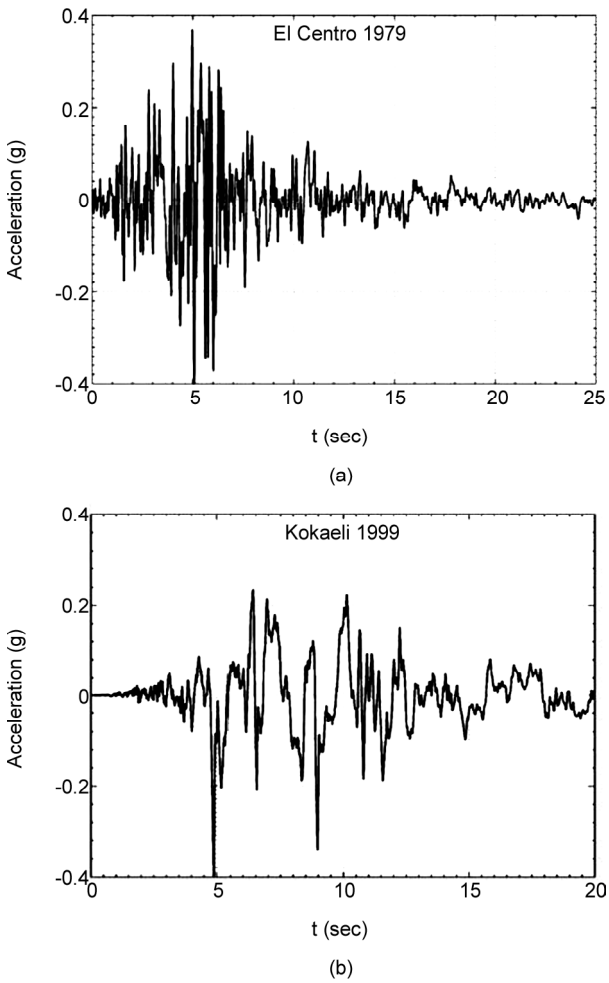

Figure 4. Acceleration history of horizontal component of (a) El Centro 1979 and (b) Kocaeli 1999.

models, damping was excluded and will be added in additional parametric studies. Input values of the program developed for MATLAB are given, Table (1). The mass of the ballast vibrating with the track system was estimated as 4.42 times larger than the track without consideration of the ballast mass. The additional mass naturally produces larger seismic loads. The parameter required for stretching the PML model is the dominant frequency of the exciting record, which can be obtained from amplitude of its Fourier transform. These values were 1.9 for the El Centro record and 0.3 Hz for Kocaeli.

The predominant frequency responses of the earthquake excitations are determined to investigate their effects on the seismic response of the system. The response acceleration spectra of the El Centro and Kocaeli excitations are 7.14 and 2.17 Hz, respectively, Figure (5).

Using the PML model, lateral response of the track is calculated at its origin, Figure (6).

The deflection amplitudes of the beam for the C1 and C2, with corresponding foundation stiffnesses and lateral loading, are shown in Table (2) along with the first natural frequency of the system.

Table (2) shows the response for C1 and C2. In C1, the first natural frequency of the beam on soft subgrade is 6.72 Hz, which is close to the predominant frequency of the El Centro ground acceleration (7.14 Hz). Consequently, the response amplitude for El Centro is 4.1 times larger than that of Kocaeli. The same value for hard subgrade is only 2.7. On the other hand for C2, the response for the El Centro record is only 1.1 that of Kocaeli in soft subgrade and 1.9 for hard subgrade. By including the additional mass of the ballast, the first natural frequency for C2 and soft subgrade is 3.19 and 9.04 for hard subgrade. It can be observed that in this case, the predominant frequency of the Kocaeli is closer to that of the track on soft subgrade as compared to that of the El Centro

Table 1. Numerical input data in PML solution of earthquake excitation.

Young's modulus (GPa)	210
Moment of inertia, I_{zz} (m^4)	1026×10^{-8}
Density per unit length of rail (kg/m)	119.87
Equivalent density per unit length of railroad (Ballast included) (kg/m) [21]	529.87
Winkler constant per unit length in soft region, k_{s1}^{z} (kN/m^2) [32]	213.5
Winkler constant per unit length in strong region, k_{s2}^{z} (kN/m^2) [32]	1708

Table 2. Maximum horizontal displacement (m) of all beam nodes under earthquake excitation for different conditions.

	C1		C2		Predominant Frequency of Excitation (Hz)
	Soft	Strong	Soft	Strong	
El Centro (1979)	0.01831	0.00101	0.06564	0.00968	7.14
Kocaeli (1999)	0.00450	0.00037	0.06121	0.00504	2.17
First natural frequency (Hz)	6.72	19.00	3.19	9.04	

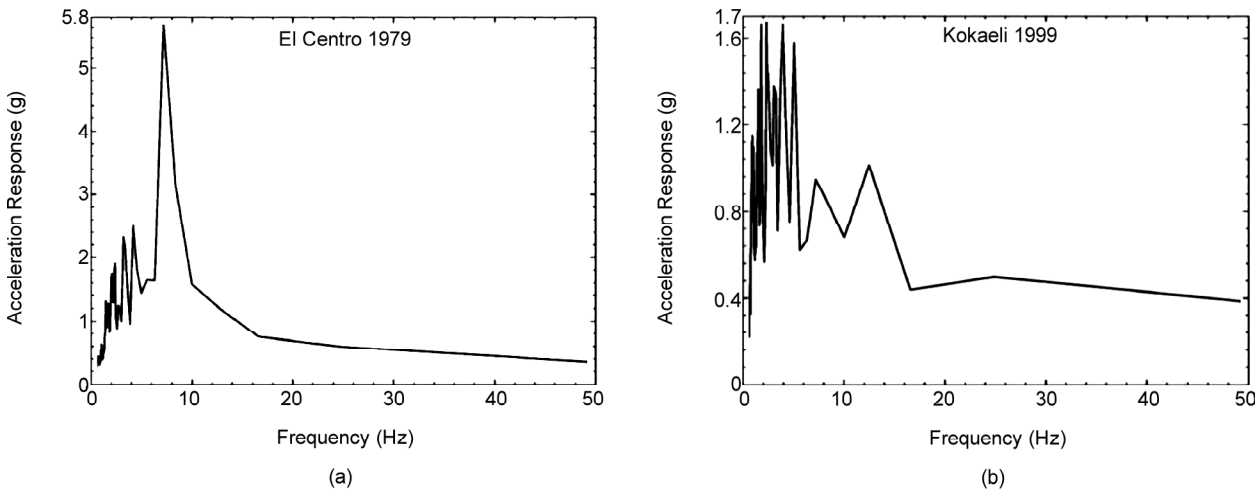

Figure 5. Acceleration response spectram of (a) El Centro 1979 and (b) Kocaeli 1999.

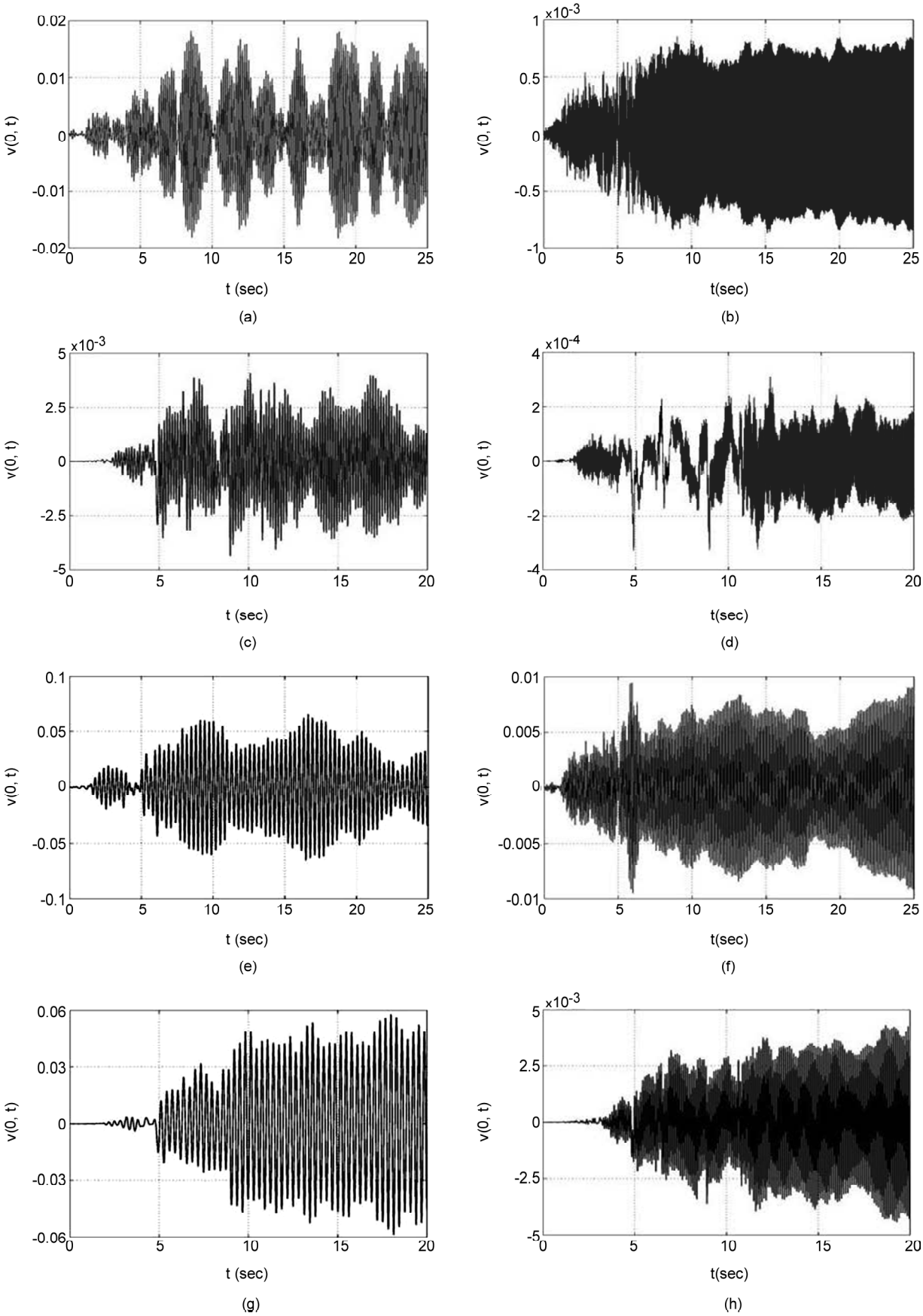

Figure 6. Displacement response of the track at the origin for different data of earthquake excitation, region and mass, respectively: (a) El Centro; soft subgrade, rail mass only (b) El Centro; hard subgrade, rail mass only (c) Kocaeli; soft subgrade, rail mass only (d) Kocaeli; hard subgrade, rail mass only (e) El Centro; soft subgrade, ballast mass included (f) El Centro; hard subgrade, ballast mass included (g) Kocaeli; soft subgrade, ballast mass included (h) Kocaeli; hard subgrade, ballast mass included.

record. This was the reverse of the results obtained for C1. Thus, by considering time domain dynamic analysis, the amplified rail response, which is the consequence of resonance phenomenon, can be computed. It can be seen that the PML approach for supported infinite beams, developed in this study, can be a useful tool for the assessment of railroad dynamic responses under earthquakes as well as for seismic vulnerability assessments.

5. Conclusions

In this study, a PML approach was used in the solution of semi-infinite Bernoulli-Euler beams on elastic foundations. The governing equations for perfectly matched medium (PMM) were obtained by modification of the beam equations for an elastic medium. This involved a continuous, complex-valued, coordinate stretching. The PMM could be interpreted as an inhomogeneous viscoelastic medium. Auxiliary differential equations (ADE) were employed in frequency domain in order to convert the fourth-order differential equation to four first-order equations. The counterpart of these equations in time domain involves convolutions. Implementation of the governing equation in displacement-based FEM, needs recasting the equations into a format that contains only displacements as unknowns. The proposed scheme produces internal moments and shear forces from ADEs. These nonlinear forces lead to a tangent mass matrix that can be incorporated into the solution along with the effective tangent stiffness matrix.

The efficiency and accuracy of the PML results were validated through a rudimentary trial-and-error procedure and by comparison with numerical solution of a long beam. The solution process can be easily applied to viscoelastic foundations, and Timoshenko beams, as well as various loading conditions. The response of railroad tracks subjected to earthquake excitations, shows its dependent on both system properties (foundation stiffness, mass) and predominant frequencies of the seismic record. Such factors can cause resonance in the track response.

References

1. Alonso-Mallo, I. and Reguera, N. (2003) Discrete absorbing boundary conditions for Schrodinger-type equations. Construction and error analysis. *SIAM Journal on numerical Analysis*, **41**(5), 1824-1850.
2. Chew W.C. (1995) *Waves and Fields in Inhomogeneous Media*. IEEE Press: Piscataway, NJ.
3. Bielak, J., Loukakis, K., Hisada, Y., and Yoshimura, C. (2003) Domain reduction method for three-dimensional earthquake modelling in localized regions, Part I: Theory. *Bulletin of the Seismological Society of America*, **93**(2), 817-824.
4. Wolf, J.P. (1985) *Dynamic Soil-Structure-Interaction*. Prentice Hall, Englewood Cliffs, NJ.
5. Wolf, J.P. (1988) *Soil-Structure-Interaction Analysis in Time Domain*. Prentice Hall, Englewood Cliffs, NJ.
6. Sun, L. (2003) An explicit representation of steady state response of a beam on an elastic foundation to moving harmonic line loads. *International Journal for Numerical and Analytical Methods in Geomechanics*, **27**, 69-84.
7. Ruge P. and Trinks C. (2004) Consistent modelling of infinite beams by fractional dynamics. *Nonlinear Dynamics*, **38**, 267-284.
8. Kargarnovin, M.H., Younesian, D., Thompson, D.J. and Jones, C.J.C. (2005) Response of beams on nonlinear viscoelastic foundations to harmonic moving loads. *Computers and Structures*, **83**, 1865-1877.
9. Ruge, P. and Birk, C.A (2007) Comparison of infinite Timoshenko and Euler-Bernoulli beam models on Winkler foundation in the frequency - and time - domain. *Journal of Sound and Vibration*, **304**, 932-947.
10. Kausel, E. (1988) Local transmitting boundaries. *Journal of Engineering Mechanics (ASCE)*, **114**, 1011-1027.
11. Beskos, D.E. (1997) Boundary element methods in dynamic analysis: Part II (1986-1996). *Applied Mechanics Reviews (ASME)*, **50**, 149-197.
12. Harari, L. (2006) A survey of finite element methods for time-harmonic acoustics. *Computer Methods in Applied Mechanics and Engineering*, **195**, 1594-1607.

13. Tianyun L. and Qingbin L. (2003) Transient elastic wave propagation in an infinite Timoshenko beam on viscoelastic foundation. *International Journal of Solids and Structures*, **40**, 3211-3228.

14. Berenger, J.P. (1994) A perfectly matched layer for the absorption of electromagnetic waves. *Journal of Computational Physics*, **114**(2), 185-200.

15. Jiong, L., Jian-wei, M., and Hui-zhu, Y. (2009) The study of perfectly matched layer absorbing boundaries for SH wave fields. *Applied Geophysics*, **6**(3), 267-274.

16. Nataf, F. (2006) A new construction of perfectly matched layers for the linearized Euler equations. *Journal of Computational Physics*, **214**(2), 757-772.

17. Komatitsch, D. and Martin, R. (2007) An unsplit convolutional perfectly matched layer improved at grazing incidence for the seismic wave equation. *Geophysics*, **72**(5), SM155-SM167.

18. Zhen, Q., Minghui, L., Xiaodong, Z., Yao, Y., Cai, Z., and Jianyong, S. (2009) The implementation of an improved NPML absorbing boundary condition in elastic wave modeling. *Applied Geophysics*, **6**(2), 113-121.

19. Martin R. and Komatitsch D. (2009) An unsplit convolution perfectly matched layer technique improved at grazing incidence for the viscoelastic wave equation. *Geophysical Journal International*, **179**(1), 333-344.

20. Martin, R., Komatitsch, D., and Ezziani, A. (2008) An unsplit convolution perfectly matched layer improved at grazing incidence for seismic wave equation in poroelastic media. *Geophysics*, **73**(4), T51-T61.

21. Basu, U. and Chopra, A.K. (2003) Perfectly matched layers for time-harmonic elastodynamics of unbounded domains: theory and finite-element implementation. *Computer Methods in Applied Mechanics and Engineering*, **192**, 1337-1375.

22. Kang, J.W. and Kallivokas, L.F. (2010) Mixed unsplit-field perfectly matched layers for transient simulations of scalar waves in heterogeneous domains. *Computational Geosciences*, **14**, 623-648.

23. Argyroudis, S. (2010) Contribution to seismic vulnerability and risk of transportation networks in urban environment. PhD Thesis, Dept. of Civil Engineering, and Aristotle University of Thessaloniki, Greece.

24. Banimahd, A. and Arbabi, F. (2012) Seismic vulnerability assessment and development of analytical fragility curves for railroads. *Journal of Seismology and Earthquake Engineering*. **4**, 251-262.

25. Esmaeili, M. and Noghabi, H.H. (2013) Investigating seismic behaviour of ballasted railway track in earthquake excitation using finite-element model in three-dimensional space. *Journal of Transportation Engineering ASCE*, **139**(7), 697-708.

26. Nakamura, T., Sekine, E., and Shirae, Y. (2011) Assessment of aseismic performance of ballasted tracks in large-scale earthquakes. *RTRI Rep.*, **52**(3), 156-162.

27. Li, L., Peng, W.T., Li, G., Chen, Y., Chen, Q.F., and Tang, Y. (2004) Vibration induced by train: a new seismic source and observation. *Chinese Journal of Geophysics*, **47**(4), 775-779.

28. Chew, W.C., Jin, J.M., and Michielssen, E. (1997) Complex coordinate stretching as a generalized absorbing boundary condition. *Microwave and Optical Technology Letters*, **15**(6), 363-369.

29. Zienkiewicz, O.C. and Taylor, R.L. (1989) *The Finite Element Method*. McGraw Hill. Vol. I. and Vol. II, (1991).

30. Boresi, A.P., Schmidt, R.J., and Sidebottom, O.M. (1993) *Advanced Mechanics of Materials*. John Wiley & Sons, Inc.

31. Zakeri, J.A., Mirfattahi, B., and Fakhari, M. (2012) Lateral resistance of railway track with frictional sleepers. *Proceedings of the Institution of Civil Engineers - Transport journal*. **165**(2), 151-155.

32. Zarfam, R. and Khaloo, A.R. (2012) Vibration control of beams on elastic foundation under a moving vehicle and random lateral excitations. *Journal of Sound and Vibration*, **331**, 1217-1232.